J|A|C|S
ARTICLES
Published on Web 05/17/2005

Gold Cluster Carbonyls: Saturated Adsorption of CO on Gold Cluster Cations, Vibrational Spectroscopy, and Implications for Their Structures

André Fielicke,[†] Gert von Helden,[†] Gerard Meijer,[†] David B. Pedersen,[‡] Benoit Simard,[‡] and David M. Rayner*[,‡]

Contribution from the Fritz-Haber-Institut der Max-Planck-Gesellschaft, Faradayweg 4-6, D-14195 Berlin, Germany, and Steacie Institute for Molecular Sciences, National Research Council, 100 Sussex Drive, Ottawa, Ontario, Canada K1A 0R6

Received February 13, 2005; E-mail: David.Rayner@nrc-cnrc.gc.ca

Abstract: We report on the interaction of carbon monoxide with cationic gold clusters in the gas phase. Successive adsorption of CO molecules on the Au_n^+ clusters proceeds until a cluster size specific saturation coverage is reached. Structural information for the bare gold clusters is obtained by comparing the saturation stoichiometry with the number of available equivalent sites presented by candidate structures of Au_n^+. Our findings are in agreement with the planar structures of the Au_n^+ cluster cations with $n \leq 7$ that are suggested by ion mobility experiments [Gilb, S.; Weis, P.; Furche, F.; Ahlrichs, R.; Kappes, M. M. *J. Chem. Phys.* **2001**, *116*, 4094]. By inference we also establish the structure of the saturated $Au_n(CO)_m^+$ complexes. In certain cases we find evidence suggesting that successive adsorption of CO can distort the metal cluster framework. In addition, the vibrational spectra of the $Au_n(CO)_m^+$ complexes in both the CO stretching region and in the region of the Au−C stretch and the Au−C−O bend are measured using infrared photodepletion spectroscopy. The spectra further aid in the structure determination of Au_n^+, provide information on the structure of the Au_n^+−CO complexes, and can be compared with spectra of CO adsorbates on deposited clusters or surfaces.

Introduction

The chemistry of gold nanoparticles exemplifies the fundamental difference between material in its bulk and in its cluster state. Whereas bulk gold is chemically inert, deposited gold nanoparticles[1−3] and clusters[4−7] can have a highly size-specific catalytic activity. A dramatic size dependence in reactivity has even been found for isolated gold clusters containing only a few atoms. [8−12]

A prototype reaction to probe the catalytic properties of Au nanoparticles is CO oxidation by molecular oxygen. The interaction of gold clusters with CO and O_2, including their independent adsorption and their coadsorption and reaction, is a very active field of experimental and theoretical research. As the properties of free clusters in the gas phase form a basis for understanding the chemistry of supported nanoparticles, it is of interest to investigate the chemistry of gas-phase gold clusters.

Size-dependent changes of cluster reactivity are normally interpreted in terms of changes in electronic and/or geometric structures.[13] Detailed structural information on small isolated cationic[14,15] and anionic[16] gold clusters has been obtained by ion mobility measurements made in conjunction with density functional theory (DFT) calculations. The Au_n^+ cations are reported to have planar structures for $n = 3-7$ and 3-D structures for $n \geq 8$ at room temperature. From measurements made at 77 K, there is evidence that Au_9^+ exists in at least two isomeric forms.[15] Other information on structures of gold clusters comes from photoelectron spectroscopy in conjunction with theory[17,18] as well as from theory alone.[19−23]

[†] Fritz-Haber-Institut der Max-Planck-Gesellschaft.
[‡] Steacie Institute for Molecular Science.

(1) Valden, M.; Lai, X.; Goodman, D. W. *Science* **1998**, *281*, 1647.
(2) Haruta, M. *Catal. Today* **1997**, *36*, 153.
(3) Shaikhutdinov, S. K.; Meyer, R.; Naschitzki, M.; Bäumer, M.; Freund, H.-J. *Catal. Lett.* **2003**, *86*, 211.
(4) Yoon, B.; Häkkinen, H.; Landman, U.; Wörz, A. S.; Antonietti, J.-M.; Abbet, S.; Judai, K.; Heiz, U. *Science* **2005**, *307*, 403.
(5) Sanchez, A.; Abbet, S.; Heiz, U.; Schneider, W.-D.; Häkkinen, H.; Barnett, R. N.; Landman, U. *J. Phys. Chem. A* **1999**, *103*, 9573.
(6) Heiz, U.; Sanchez, A.; Abbet, S.; Schneider, W.-D. *Chem. Phys.* **2000**, *262*, 189.
(7) Häkkinen, H.; Abbet, S.; Sanchez, A.; Heiz, U.; Landman, U. *Angew. Chem., Int. Ed.* **2003**, *42*, 1297.
(8) Lee, T. H.; Ervin, K. M. *J. Phys. Chem.* **1994**, *98*, 10023.
(9) Wallace, W. T.; Whetten, R. L. *J. Phys. Chem. B* **2000**, *104*, 10964.
(10) Hagen, J.; Socaciu, L. D.; Elijazyfer, M.; Heiz, U.; Bernhardt, T. M.; Wöste, L. *Phys. Chem. Chem. Phys.* **2002**, *4*, 1707.
(11) Socaciu, L. D.; Hagen, J.; Bernhardt, T. M.; Wöste, L.; Heiz, U.; Häkkinen, H.; Landman, U. *J. Am. Chem. Soc.* **2003**, *125*, 10437.
(12) Kimble, M. L.; Castleman, A. W., Jr.; Mitrić, R.; Bürgel, C.; Bonačić-Koutecký, V. *J. Am. Chem. Soc.* **2004**, *126*, 2526.
(13) Knickelbein, M. B. *Annu. Rev. Phys. Chem.* **1999**, *50*, 79.
(14) Gilb, S.; Weis, P.; Furche, F.; Ahlrichs, R.; Kappes, M. M. *J. Chem. Phys.* **2001**, *116*, 4094.
(15) Weis, P.; Bierweiler, T.; Vollmer, E.; Kappes, M. M. *J. Chem. Phys.* **2002**, *117*, 9293.
(16) Furche, F.; Ahlrichs, R.; Weis, P.; Jacob, C.; Gilb, S.; Bierweiler, T.; Kappes, M. M. *J. Chem. Phys.* **2002**, *117*, 6982.
(17) Li, J.; Li, X.; Zhai, H. J.; Wang, L.-S. *Science* **2003**, *299*, 864.
(18) Häkkinen, H.; Yoon, B.; Landman, U.; Li, X.; Zhai, H.-J.; Wang, L.-S. *J. Phys. Chem. A* **2003**, *107*, 6168.
(19) Grönbeck, H.; Andreoni, W. *Chem. Phys.* **2000**, *262*, 1.
(20) Häkkinen, H.; Landman, U. *Phys. Rev. B* **2000**, *62*, R2287.
(21) Bonačić-Koutecký, V.; Mitrić, R.; Ge, M.; Zampella, G.; Fantucci, P. *J. Chem. Phys.* **2002**, *117*, 3120.

10.1021/ja0509230 CCC: $30.25

Here, we focus on the adsorption of CO on small cationic gold clusters. From a fundamental viewpoint, the CO ligand can be used to probe electronic and geometric structure in both free and supported Au nanoparticles. Comparing the properties of clusters in the different environments can contribute to determining support effects. The interaction of CO with gold clusters has been studied in the gas phase using flow reactor and ion trap techniques.[8,9,24−27] A review concentrating on small clusters has appeared recently.[28] Reaction rates have been measured for the addition of CO to small cluster anions.[8,26] Saturation CO uptake on the gold cluster anions suggests that adsorption is controlled by electron shell filling rather than by any obvious geometric considerations.[9,27] The reactions of CO with neutral and cationic clusters are less well studied. The neutral dimer is known to react to form Au_2CO with a binding energy of >25 kcal mol^{-1}.[29] For the cations, there has been a short report describing an ion trap collision induced dissociation experiment that found CO to bind especially strongly to Au_7^+ and Au_{19}^+.[25] A recent, more comprehensive study, measured the kinetics of single CO addition to Au_n cations up to $n = 66$ in an ion cyclotron resonance mass spectrometer and applied a radiative association model to extract binding energies. This study showed that the binding energies decrease relatively smoothly with increasing cluster size, from about 1.09 ± 0.1 eV at $n = 6$ to below 0.65 ± 0.1 eV at $n = 66$.[30] Vibrational spectroscopy of the CO ligand can complement these measurements of kinetic and thermochemical reaction data to give valuable information about the geometry of the binding site and about the electron density at the metal.

Here, we report on the formation of cationic gold cluster carbonyls and on the vibrational spectroscopy of the CO ligands in these carbonyls. The saturation CO uptake is measured for cationic gold clusters. From the stoichiometries of the saturated cluster carbonyls $Au_n(CO)_m^+$, information on the structure of the metal cluster core can be inferred by comparison with the number of available (equivalent) adsorption sites present in candidate structures for Au_n^+. Using infrared photodepletion spectroscopy, we measure the vibrational spectra of these complexes in both the CO stretching region as well as in the region of the Au−C stretch and the Au−C−O bend. These vibrational spectra give further aid in the geometric structure determination of the clusters.

Experimental Section

The experiments are carried out in a cluster beam apparatus that has been described before.[31−33] Gold cluster cations are generated and entrained in a flow of He in a pulsed laser ablation cluster source. They pick up CO, delivered through a second pulse valve in a small reactor channel before expanding to produce a beam of $Au_n(CO)_m^+$ species. The extent of CO-complex formation is controlled by adjusting the CO flow through the second valve. The beam passes through a skimmer to the detection chamber where the cations are detected using a pulsed-field-extraction time-of-flight mass spectrometer (TOFMS). The IR beam counter propagates the cluster beam and is loosely focused to fill an aperture through which the cluster beam enters the ion detection region of the TOFMS. This ensures that the full cross-section of the cluster beam entering the TOFMS is exposed to the IR laser beam.

IR light is generated by the Free Electron Laser for Infrared eXperiments (FELIX).[34] This FEL delivers continuously tunable macropulses of infrared radiation, 6−8 μs in duration, at a repetition rate of 5 Hz. Each macropulse consists of a 1 GHz train of micropulses of typically 2 ps duration. For the experiments reported here the macropulse energy was ~7 mJ at 2000 cm^{-1} and 60 mJ at 300 cm^{-1} corresponding to micropulse energies of ~1 and ~10 μJ, respectively. In the ν(CO) stretching region FELIX frequencies are calibrated by recording the infrared absorption spectra of ethylene and CO in a photoacoustic cell. At lower frequencies, in the range of 250−400 cm^{-1}, the frequencies are calibrated using a grating spectrometer. The bandwidth of the IR laser radiation is measured on the Q-branch of the $\nu_7 + \nu_8$ combination band of ethylene to be 10−20 cm^{-1} at 1890 cm^{-1}, limited by the micropulse length of FELIX. In the low-frequency range, the bandwidth is ~0.5% of the central frequency (typically 2 cm^{-1}). We estimate that the absolute accuracy of the wavenumber scale is about 2 cm^{-1} in the investigated frequency range.

The TOFMS extraction pulse is timed to collect ions from the portion of the beam exposed to FELIX. Infrared spectra are measured by recording mass spectra while the wavelength of FELIX is stepped. Reference mass spectra, with the IR pulse turned off, are recorded on alternate shots to compensate for any drift in the cluster beam intensity. The IR depletion spectra are subsequently constructed by integrating the signal intensity corresponding to a certain complex for each wavelength.

Results and Discussion

Composition of Saturated Cationic Gold Cluster Carbonyls. A mass spectrum of gold cluster cations produced by the ablation source is shown in Figure 1a. When CO is added via a pulsed valve into the flow reactor, complexes of the gold cluster cations with CO are formed. By increasing the backing pressure of the CO, the carbonyl formation proceeds by successive addition of single CO ligands (Figure 1b) to the point where the clusters saturate, as demonstrated by the pile-up at specific complex stoichiometries in Figure 1c and by the uptake plots shown in Figure 2. In these uptake plots, the intensities of selected gold cluster carbonyls are plotted as a function of the CO backing pressure. Although the absolute partial pressure of the CO in the reaction channel is unknown, the intensity dependencies of the intermediate and final products on the CO addition strongly resemble those of a successive addition mechanism. At higher CO pressures the intermediate adducts vanish and the mass spectrum is dominated by the signals of saturated cationic gold cluster carbonyls. The masses of these gold carbonyls correspond to the species $Au_3(CO)_3^+$, $Au_4(CO)_4^+$, $Au_5(CO)_{4/5}^+$, $Au_6(CO)_{5/6}^+$, $Au_7(CO)_6^+$, $Au_8(CO)_7^+$, $Au_9(CO)_8^+$, and $Au_{10}(CO)_6^+$.

In previous studies it has been found that saturated adsorption of CO on the surface of metal clusters may not only be determined by electronic effects but can also be dependent on

(22) Wang, J.; Wang, G.; Zhao, J. *Phys. Rev. B* **2002**, *66*, 035418.
(23) Wells, D. H., Jr.; Delgass, W. N.; Thomson, K. T. *J. Chem. Phys.* **2002**, *117*, 10597.
(24) Cox, D. M.; Brickman, R.; Creegan, K.; Kaldor, A. *Z. Phys. D* **1991**, *19*, 353.
(25) Nygren, M. A.; Siegbahn, P. E. M.; Jin, C.; Guo, T.; Smalley, R. E. *J. Chem. Phys.* **1991**, *95*, 6181.
(26) Balteanu, I.; Balaj, O. P.; Fox, B. S.; Beyer, M. K.; Bastl, Z.; Bondybey, V. E. *Phys. Chem. Chem. Phys.* **2003**, *5*, 1213.
(27) Wallace, W. T.; Whetten, R. L. *Eur. Phys. J. D* **2001**, *16*, 123.
(28) Bernhardt, T. M. *Int. J. Mass Spectrosc.* **2005**, *243*, 3.
(29) Lian, L.; Hackett, P. A.; Rayner, D. M. *J. Chem. Phys.* **1993**, *99*, 2583.
(30) Neumaier, M.; Weigend, F.; Hampe, O.; Kappes, M. M. *J. Chem. Phys.* **2005**, *122*, 104702.
(31) von Helden, G.; van Heijnsbergen, D.; Meijer, G. *J. Phys. Chem. A* **2003**, *107*, 1671.
(32) Simard, B.; Dénommée, S.; Rayner, D. M.; van Heijnsbergen, D.; Meijer, G.; von Helden, G. *Chem. Phys. Lett.* **2002**, *375*, 195.
(33) Fielicke, A.; von Helden, G.; Meijer, G.; Pedersen, D. B.; Simard, B.; Rayner, D. M. *J. Phys. Chem. B* **2004**, *108*, 14591.
(34) Oepts, D.; van der Meer, A. F. G.; van Amersfoort, P. W. *Infrared Phys. Technol.* **1995**, *36*, 297.

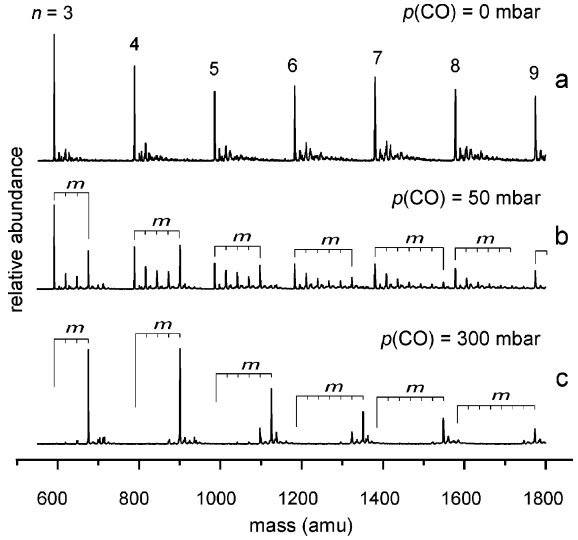

Figure 1. Mass spectra of $Au_n(CO)_m^+$ cluster complexes showing saturation at high CO flow rates: (a) spectrum of Au_n^+ clusters in the absence of CO; (b) spectrum at intermediate flow rate (backing pressure at the CO inlet valve = 50 mbar) showing sequential addition of CO; (c) saturated spectrum observed with a backing pressure of 300 mbar. The scales above the spectra mark the expected positions of the parent Au_n^+ cluster peaks and the expected positions as CO is added.

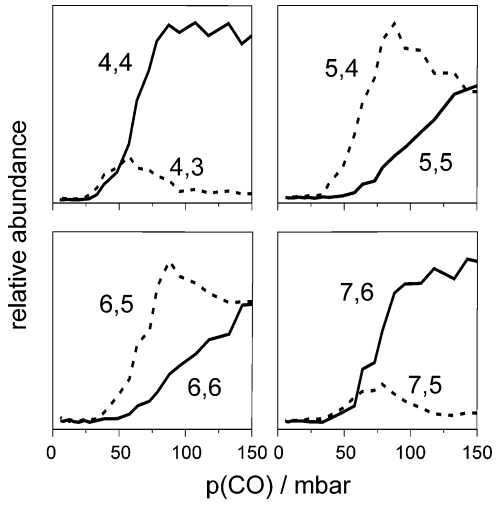

Figure 2. Dependence of the abundance of selected $Au_n(CO)_m^+$ complexes (labeled as *n*, *m*) on the relative partial pressure of CO in the reactor as determined by the backing pressure behind the pulsed valve.

the geometric structures of the metal clusters and can thus be used to determine the structure of the clusters.[35,36] In the following, we discuss implications for the structures of the gold clusters that can be derived from the observed compositions of the saturated cluster carbonyls. Figure 3 shows several candidate structures for Au_n^+ clusters arising from the recent ion mobility and DFT studies.[14] Atop adsorption (i.e. coordination to a single Au atom) is expected from DFT studies of single CO molecules binding to Au cluster cations.[37] For $n = 3$, 4, 7, 8, and 9 the number of CO molecules bound at saturation, $m_{sat.}$, is clearly consistent with CO occupying all available atop sites on the edge Au atoms of the planar structures (see Figure 3).

For Au_5^+ and Au_6^+ the clusters quickly add four and five COs, respectively, but go on to add an extra CO more slowly

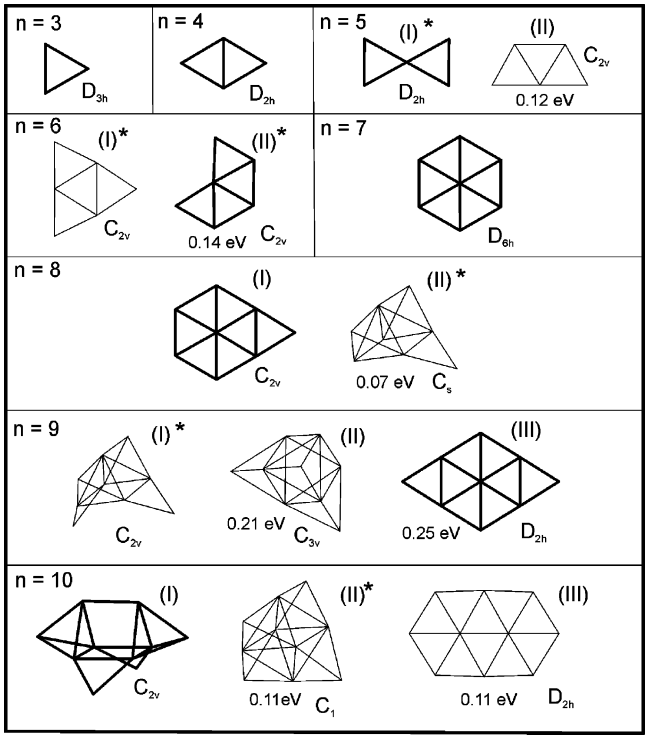

Figure 3. Structures of cationic gold clusters. The underlying structures are taken from the DFT results of ref 14. Structures consistent with our CO uptake measurements are drawn in bold. Where there is no ambiguity between the DFT calculations, the ion mobility measurements of ref 14 and our CO uptake measurements, only a single structure is given. Where more than one structure is given, the lowest energy form calculated by DFT is labeled (I) and the relative energy of the higher energy structures is noted. In this case, an asterisk is used to denote the structure deduced from the ion mobility measurements.

at higher CO pressure (Figure 2). Kinetic modeling shows that the *p*(CO) dependence is consistent with a sequential addition reaction rather than with the presence of two cluster isomers reacting independently. The initial $m_{sat.}$ value of 4 for Au_5^+ is fully consistent with the D_{2h} X-shaped structure, 5(I), favored by both ion mobility measurements and DFT, under the assumption that the central 4-fold cooordinated Au atom is not reactive. For Au_6^+, the ion mobility measurements could not distinguish between the two structures 6(I) and 6(II) because of their similar cross-sections, although DFT favored the distorted D_{3h} triangular structure by 0.14 eV. Our initial value of $m_{sat} = 5$ favors structure 6(II), assuming that the central Au atom in this structure (with five neighbored Au atoms) is unreactive toward CO. It is possible that the slower addition of an extra CO to both $Au_5(CO)_4^+$ and $Au_6(CO)_5^+$ involves addition to the more highly coordinated central Au atom. Another possibility is that it is the result of a structural change in the cluster, driven and stabilized by the addition of CO. Structural changes in the metal cluster framework as CO coverage reaches saturation is already well documented in smaller Ni cluster CO complexes ($n \leq 13$). The adsorption energy for a single CO on Au_6^+ is experimentally found to be ~1.1 eV. [30] This is several times the difference in energies between structures (I) and (II) for both Au_5^+ and Au_6^+ and may well be sufficient to overcome the barriers for structural change

(35) Parks, E. K.; Kerns, K. P.; Riley, S. J. *J. Chem. Phys.* **2000**, *112*, 3384.
(36) Kerns, K. P.; Parks, E. K.; Riley, S. J. *J. Chem. Phys.* **2000**, *112*, 3394.
(37) Wu, X.; Senapati, L.; Nayak, S. K.; Selloni, A.; Hajaligol, M. *J. Chem. Phys.* **2002**, *117*, 4010.

to accommodate an extra CO. The final compositions $Au_5(CO)_5^+$ and $Au_6(CO)_6^+$ would be in agreement with saturated carbonyls of 5(II) and 6(I). In those complexes, the CO binds to gold atoms having between two and four neighboring gold atoms. It is also possible that the clusters could adopt three-dimensional structures on taking up the final CO. For the bare Au_5^+ and Au_6^+ clusters the lowest 3-D structures lie as low as 0.45 eV above the ground state according to DFT. The lowest 3-D structure for Au_5^+ is a distorted trigonal bipyramid. In this structure and in the other low-lying 3-D structures of Au_5^+ and Au_6^+ all the gold atoms have four or less neighboring gold atoms.

For Au_8^+ and Au_9^+ our $m_{sat.}$ values of 7 and 8, respectively, are, at first sight, consistent with either the 3-D structures indicated by the ion mobility study, 8(II) and 9(I), or the planar structures, 8(I) and 9(III). The 3-D 9(II) is not compatible with $m_{sat} = 8$ as it has three equivalent six-coordinated, three equivalent five-coordinated, and three equivalent three-coordinated Au sites. The saturation values of $m_{sat.} = 7$ and 8 could be explained by the presence of the 3-D structures 8(II) and 9(I), although this requires that CO does not bind to the single six-coordinated Au site found in both structures, but that it does bind easily to the five-coordinated sites. However, it will be shown below that CO does not bind to Au atoms with more than four neighbored gold atoms. Therefore, the saturation values favor the planar clusters 8(I) and 9(III) as the core structures of $Au_8(CO)_7^+$ and $Au_9(CO)_8^+$, respectively. Note that we do not challenge the structures for the bare clusters revealed by the mobility measurements but propose that the CO adsorption energy again drives structural change in the clusters. In the case of the octamer the DFT study found the planar structure 8(I) to be 0.06 eV lower than the 3-D structure 8(II), whereas for the nonamer the planar structure 9(III) is found 0.25 eV higher in energy than the 3-D structure 9(I). A simple unfolding motion of 8(II) and 9(I) leads directly to the planar structures for $n = 8$ and 9. Rapid isomerization of the nonamer between the structures 9(I) and 9(II) has been observed at temperatures as low as 140 K in temperature-dependent ion mobility measurements.[15] From the temperature dependence the barrier to interconversion is estimated to be between 0.1 and 0.2 eV, actually less than the energy difference calculated by DFT. CO addition could easily drive the structure over much higher barriers. We will return to this discussion following our presentation of the vibrational spectra.

A break in the saturation behavior comes at $n = 10$ where there is a metastable saturation when $m_{sat.}$ is only 6 (further CO ligands bind sequentially at higher CO pressures). Structure 10(I), slightly favored by DFT but not by ion mobility, is the only candidate consistent with this value. It has four Au atoms that are five-coordinated and will give $m_{sat.} = 6$ if CO only binds at sites with lower coordination. This suggests that Au_{10}^+ is 3-D and that the barrier for reaching the planar 10(III) is high enough to prevent its formation despite it being only 0.11 eV above the 3-D 10(I) lowest energy structure. A higher barrier is reasonable for Au_{10}^+, compared to Au_9^+, as the reorganization to form the D_{2h} planar structure is more complex and involves the breaking of several more Au−Au bonds. The apparent low CO binding energy for five-coordinated Au atoms, for the six-coordinated atom on 3-D 8(II) and 9(I) and for the central atoms of the planar structures that correspond to pieces of the Au(111) surface is consistent with the inability of CO to bind to Au(111) surfaces at room temperature.

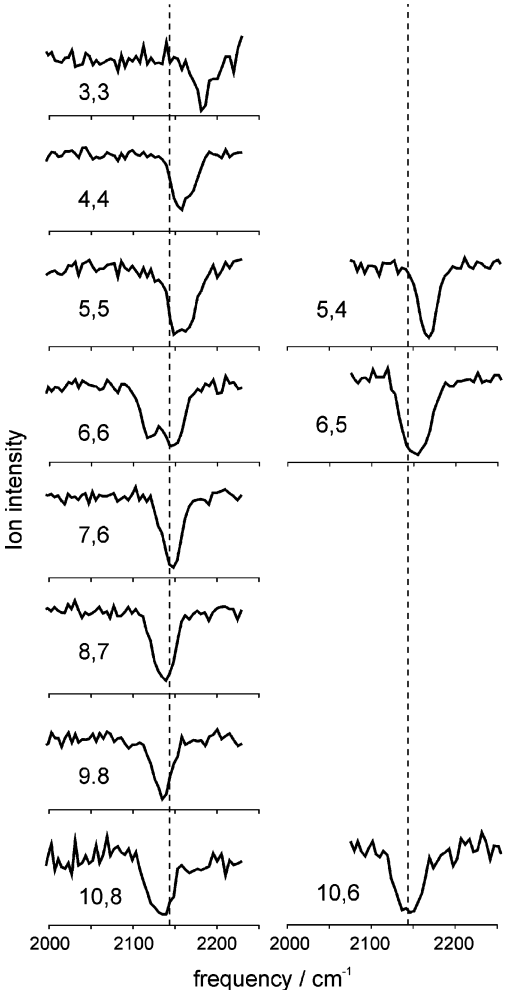

Figure 4. IR-MPD spectra of $Au_n(CO)_m^+$ complexes, identified by the label *n*, *m*, in the spectral region around ν(CO). The relative depletion of the ion signal is plotted versus the IR frequency. The spectra in the right-hand column relate to the species having at the applied CO flow the highest CO coverage; i.e. they are not distorted by growth due to the dissociation of clusters with higher values of *m*. The spectra in the left-hand column have been collected at higher CO flow in order to obtain also the spectra of the species that show two-step saturation. The vertical dotted lines mark the position of ν(CO) in free CO.

Vibrational Spectrocopy in the CO Stretching Region. The infrared depletion spectra of the CO saturated $Au_n(CO)_m^+$ complexes in the CO stretching region are shown in Figure 4. When the IR laser is on a resonance, we observe fragmentation of the complexes involving loss of several CO molecules. All spectra are collected with FELIX attenuated by 8 dB in order to avoid spectral broadening. Under those conditions, parent clusters can be depleted by 70−80%. Experimental values for ν(CO) extracted from these spectra are listed in Table 1. We find ν(CO) to be in the range of 2120−2182 cm^{-1}. These high values of ν(CO) are a characteristic of CO ligands that are atop bound at single gold atom sites in all the complexes (see below). In comparison, we measured ν(CO) for atop bound CO on cationic rhodium clusters in the range of 2050 cm^{-1} for similar-sized clusters with μ^2 bridged bound CO adsorbing at ∼100 cm^{-1} lower frequencies.[33] For the gold carbonyls, atop binding is already implied by the correlation between the saturation CO uptake and the number of available atop sites in each cluster,

Table 1. CO Vibrational Frequencies, ν(CO), in $Au_n(CO)_m^+$ Complexes in the Gas Phase[a]

n, m	ν(CO)/cm^{-1}	*n, m*	ν(CO)/cm^{-1}
3, 3	2182	7, 6	2147
4, 4	2156, 2167(sh)	8, 7	2137
5, 4	2168	9, 8	2135
5, 5	2150, 2164	10, 8	2135
6, 5	2152	10, 6	2144
6, 6	2120, 2148		

[a] The estimated uncertainty of the frequencies is ± 2 cm^{-1}.

but there are some clusters where the number of available bridging sites is the same as the number of available atop sites, making the correlation somewhat ambiguous. Our observed ν(CO) frequencies are close to what is expected from DFT calculations for a single CO adsorbed on Au cluster cations by Wu et al.,[37] who found that atop adsorption is most favorable, with ν(CO) ranging from 2200 cm^{-1} for the dimer to 2160 cm^{-1} for $n = 6$, and by Neumaier et al.[30] who report similar results but with ν(CO) $\sim$20 cm^{-1} lower. For the atom complex, $AuCO^+$, in a neon matrix ν(CO) is measured to be 2237 cm^{-1}.[38]

The number of CO stretching bands and their observed line shapes give direct information on the structures of the $Au_n(CO)_m^+$ complexes. D_{3h} $Au_3(CO)_3^+$, D_{2h} $Au_5(CO)_4^+$, and D_{6h} $Au_7(CO)_6^+$ all have only one unique type of edge atop CO binding site. They are therefore expected to exhibit a single IR active ν(CO) absorption. Indeed, relatively narrow ν(CO) bands having $\Delta\nu$ close to the bandwidth of FELIX (20 cm^{-1}) are observed for $Au_3(CO)_3^+$, $Au_5(CO)_4^+$, and $Au_7(CO)_6^+$, consistent with the structures already indicated by both our CO saturation measurements and the mobility experiments shown in Figure 3. The spectrum for $Au_4(CO)_4^+$ has a main peak at 2155 cm^{-1} with a shoulder at 2175 cm^{-1}. We attribute this double structure to the presence of two different CO binding sites on D_{2h} $Au_4(CO)_4^+$, namely, the Au atoms on the long and short diagonal axes, in agreement with the ion mobility experiments and DFT calculations on Au_4^+. The first site has the Au atom bound to two other Au atoms; the second, to three. We can expect different CO bonding at the two-coordinated and three-coordinated atoms leading to slightly different C−O stretch force constants. In addition the (CO)(CO) interaction parameters are likely to be different across the long and short diagonals, and perhaps strong enough, to induce observable splittings. $Au_5(CO)_5^+$, $Au_6(CO)_5^+$, $Au_{10}(CO)_6^+$, and $Au_{10}(CO)_8^+$ all have relatively broad ν(CO) absorption peaks that can be attributed to their having more than one distinct type of binding site in accordance with the structures suggested in Figure 3. $Au_6(CO)_6^+$ shows two resolved peaks at 2150 and 2120 cm^{-1} of about equal intensity. As discussed above, the uptake of six CO molecules suggests that the Au cluster adopts the nearly D_{3h} triangular C_{2v} structure in this complex. This structure has two distinct CO binding sites, one at the two-coordinated apex Au atoms and the second at the four-coordinated side Au atoms, consistent with the two observed ν(CO) peaks.

Vibrational Spectrocopy in the Au−C Stretching and Au−C−O Bending Region. The infrared depletion spectra of the CO saturated $Au_n(CO)_m^+$ complexes in the Au−CO stretching and Au−C−O bending region are shown in Figure 5. Scans were taken over the range from 200 to 580 cm^{-1}, but spectra

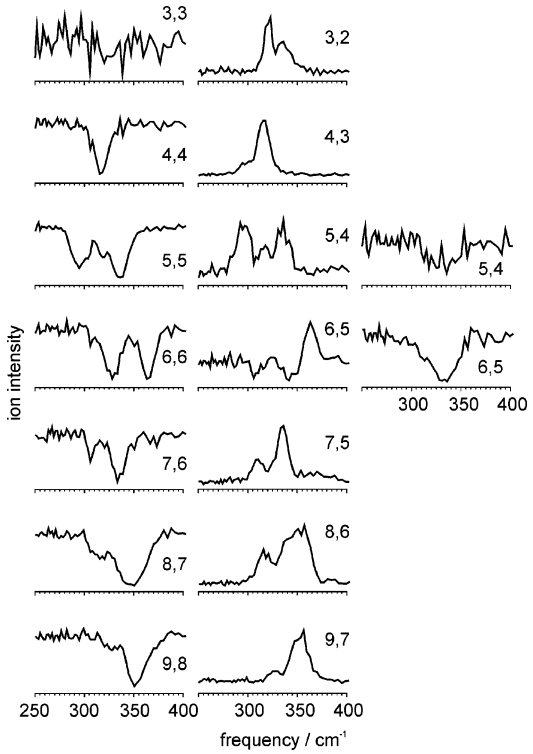

Figure 5. IR-MPD spectra of $Au_n(CO)_m^+$ complexes, identified by the label *n, m*, in the spectral region of the ν(Au−C) stretching and δ(Au−C−O) bending vibrational modes. The left-hand column shows the relative depletion of the saturated species observed under high CO flow conditions. The central column shows the related growth of the $Au_n(CO)_{m-1}^+$ signal under the same CO conditions. As justified in the text, the $Au_3(CO)_2^+$ growth can be taken as the inverse of the absorption spectrum of $Au_3(CO)_3^+$. The spectra in the right-hand column have been collected at lower CO flow in order to obtain the spectra of the species that show two-step saturation.

are only presented for the 250−400 cm^{-1} range where absorption was observed. The right- and left-hand columns in the figure give the depletion spectra of the saturated complexes. The central column shows the related growth of the $Au_n(CO)_{m-1}^+$ signal under the same CO conditions as the left-hand column. These growth spectra have better signal-to-noise than the depletion spectra because they are zero-baseline measurements, although care has to be taken in interpreting growth spectra if the fragmenting species is uncertain. They are included here because they provide the absorption spectrum of $Au_3(CO)_3^+$, even though there was insufficient absorption in this species to observe its spectrum in depletion,[39] and because they provide insight into the relative CO binding energies for some of the complexes. In the measurements, a high CO flow means that, except for $n = 5$ and 6, the CO coverage is well saturated and that there is less than 5% of the related $Au_n(CO)_{m-1}^+$ species present in the absence of IR irradiation. In contrast to our findings for the IR-MPD in the ν(CO) range, we do not observe the formation of $Au_n(CO)_{m-2}^+$ in the lower frequency range; i.e., we are only able to remove a single CO ligand. This is

(38) Liang, B.; Andrews, L. *J. Phys. Chem. A* **2000**, *104*, 9156.

(39) Three factors lower the depletion efficiency for smaller complexes. (I) The density of states drops with cluster size. As IRMPD requires coupling to a quasi-continuum of internal states, its efficiency drops for small species. (II) The multiphoton cross-section increases with the size of the complexes. Obviously it depends on the number of CO chromophores on the cluster. It is therefore easier to deplete saturated clusters than complexes with only one CO, and it is easier to deplete larger complexes than small ones. Additionally the IR intensities can increase with metal cluster size as has been calculated for the monocarbonyl complexes by Neumeier et al.[30] (III) The CO binding energy increases as the cluster size decreases, requiring the absorption of more photons to drive the dissociation.

caused by the smaller absorption cross-sections and the lower photon energies in this range, which limit the absorbed energy and thus the amount of (instantaneous or consecutive) fragmentation. Under the conditions of single CO ligand loss and low initial concentration of $Au_n(CO)_{m-1}^+$, its growth spectra correspond directly to the absorption spectra of the $Au_n(CO)_m^+$ species, as it is evident for $n = 4, 7, 8, 9$ in Figure 4. Comparison of mass spectral abundances shows that the correspondence is quantitative. For $Au_3(CO)_2^+$ the maximum growth amounts to 5% of the initial $Au_3(CO)_3^+$ signal. We are not able to observe 5% depletion at the signal-to-noise ratio of the depletion measurement but, in this case, can rely on the growth spectrum of $Au_3(CO)_2^+$ to provide the absorption spectrum of $Au_3(CO)_3^+$.

When obtaining the spectra in Figure 5 the relative amounts of $Au_5(CO)_5^+$ and $Au_5(CO)_4^+$, and the relative amounts of $Au_6(CO)_6^+$ and $Au_6(CO)_5^+$ were about equal. This causes distortion of the spectrum of $Au_6(CO)_5^+$ as clusters are not only generated but also depleted by IR-MPD. As a consequence, in the spectrum of $Au_6(CO)_5^+$ only one growth peak is observed while the dissociation spectrum of $Au_6(CO)_6^+$ shows two prominent dips. Growth of the peak at 320 cm^{-1} is apparently balanced by depletion of the initially present $Au_6(CO)_5^+$ to $Au_6(CO)_4^+$. In contrast, $Au_6(CO)_5^+$ does not absorb at 360 cm^{-1}, where the other prominent $Au_6(CO)_6^+$ absorption is. The depletion spectrum of $Au_6(CO)_5^+$, obtained at lower CO flow and shown in the left-hand column in Figure 4, confirms this. On the other hand, the growth spectrum of $Au_5(CO)_4^+$ almost matches the $Au_5(CO)_5^+$ depletion spectrum except that the relative heights of the two peaks at 290 and 330 cm^{-1} are reversed. This implies some direct depletion of the initially present $Au_5(CO)_4^+$ at ~330 cm^{-1}, but not much. This is borne out by direct measurement of the $Au_5(CO)_4^+$ depletion spectrum at lower CO flow where we observe a significantly smaller depletion yield than observed for $Au_6(CO)_5^+$ or for the other complexes except $Au_3(CO)_3^+$. The implication is that CO might be stronger bound in $Au_5(CO)_4^+$ compared to the other complexes. As in the ν(CO) range, the strong differences between the IR spectra of $Au_5(CO)_4^+$ and $Au_5(CO)_5^+$ as well as between $Au_6(CO)_5^+$ and $Au_6(CO)_6^+$ are an indication for a major change of the gold cluster structure.

The spectra in this low-frequency range show more structure than observed in the CO stretching region. Observation of this structure is helped by the higher resolution of the experiment at lower frequencies. In this range, the spectra might contain contributions from both Au−C stretching and Au−C−O bending vibrations. DFT calculations for Au_nCO^+ find values for the ν(MC) stretches of 400, 392, 403, and 367 cm^{-1} for $n =$ 3−6 in that order.[37] Evidence for the contribution of both Au−C stretching and Au−C−O bending vibrations to the observed bands can be derived from symmetry considerations. For example, for $Au_3(CO)_3^+$ and $Au_7(CO)_6^+$, the bare Au_n^+ clusters are identified by the ion mobility measurements, DFT calculations, and the CO saturation as highly symmetrical D_{nh} species (see above). The saturated complexes possessing the same symmetries should each only present a single IR active vibrational mode associated with the Au−C stretch and two IR-active modes associated with Au−C−O bending motions. In D_{3h} $Au_3(CO)_3^+$ these are identified with the E' asymmetric Au−C stretching and the E' in-plane and A_2'' out-of-plane Au−C−O bending modes. If the in- and out-of-plane bending force constants and/or interaction parameters have different values, as for example found for the equatorial MCO bonds in $Fe(CO)_5$, two absorptions should be associated with the bending modes and they might be distinguishable. In D_{6h} $Au_7(CO)_6^+$ the IR-active modes correspond to the E_{1u} asymmetric Au−C stretch and the E_{1u} in-plane and A_2'' out-of-plane Au−C−O bending modes. The presence of two peaks in the spectra of both $Au_3(CO)_3^+$ and $Au_7(CO)_6^+$ in this region indicates that either the Au−C stretch and the Au−C−O are both intense enough to be observed and the in- and out-of-plane splitting is below our resolution or that the Au−C stretching mode is insufficiently intense to be observed via multiphoton depletion and that the two peaks relate to the E and A bending modes. Force field calculations show that both types of bands can be expected to be observed in this range if the force constants for the Au−C stretch and Au−C−O bend are somewhat lower (~70%) than the related force constants in the saturated carbonyls $Fe(CO)_5$ and $Cr(CO)_5$.

The spectra of $Au_5(CO)_5^+$, $Au_6(CO)_6^+$, and $Au_8(CO)_7^+$ are expected to be more complex due to the presence of at least two different binding sites and prove to be so. $Au_4(CO)_4^+$ also has two different binding sites. In the depletion spectrum in the Au−C stretch/Au−C−O bend region there only appears to be one peak; however, the $Au_4(CO)_3^+$ growth spectrum shows a shoulder that is presumably masked in the depletion spectrum. At this point a more detailed analysis is not possible and will need more theoretical input.

$Au_9(CO)_8^+$ unexpectedly shows only a single, near-laser bandwidth limited absorption peak in the ν(CO) region and only a single peak, with perhaps a small shoulder apparent in the growth peak of $Au_9(CO)_7^+$, in the ν(AuC) stretching and δ(AuCO) bending region of the spectrum. This behavior would be more typically expected for a high-symmetry species rather than for the structures suggested by the ion mobility experiments and DFT studies or by the saturation at $m = 8$. In addition there is the evidence from ion mobility measurements that Au_9^+ exists as the two distinct isomers 9(I) and 9(II) that rapidly interconvert at temperatures as low as 140 K. If there is not fortuitous overlap in the infrared absorptions in both regions of the spectrum, we raise the possibility that the relative simplicity of the spectra is due to multiple CO addition forcing the cluster structure to a single favored isomer. Of the candidates identified by DFT theory this could be either the 3-D C_{2v} 9(I) or the planar D_{2h} 9(III) structure. On the basis of our saturation measurements, the planar form (see above) as the structure of the cluster core in $Au_9(CO)_8^+$ seems more likely. If this is the case, the relatively simple IR spectrum can be at least partially attributed to the dominance of the four equivalent CO ligands bound at the four-coordinated sites.

CO Bonding to Au Centers in Free Cationic Clusters, Surfaces, and Supported Clusters. As seen in Figure 4 and Table 1, ν(CO) for CO adsorbed on Au cluster cations generally decreases with cluster size. This is consistent with what is known about CO bonding to cationic gold centers. Usually, the metal carbonyl bond is described by an interaction of the filled σ_s* orbital of the CO with an empty, symmetry compatible metal orbital, and the back-donation from filled d-type orbitals of the metal into the empty π* orbitals of the CO. The back-donation effectively weakens the CO bond and leads to decreases in the ν(CO) stretching frequency. However, in contrast to most other

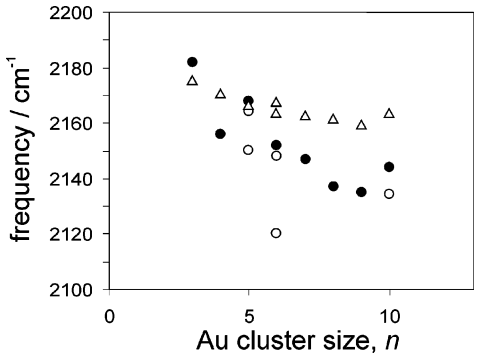

Figure 6. CO stretching frequencies, ν(CO), in saturated $Au_n(CO)_m^+$ complexes. (●, ○) Experimental values of ν(CO); see Table 1 for the values of *m*. Where results are available for two values of *m*, the higher value of *m* is depicted by an open circle. $Au_5(CO)_5^+$ and $Au_6(CO)_6^+$ exhibit two peaks. (△) ν(CO) estimated from electrostatic model calculations.

transition metals the d-shell is closed and lowered in energy and consequently appears to be less important for the bonding in gold carbonyls. This is reflected in the blue shift of ~100 cm^{-1} in cations of gold clusters compared to rhodium.[33] In the case of charged centers, a polarization effect influences the CO bond strength: on positively charged metal centers the electric field opposes the polarization of the bonding orbitals of CO. This leads to a strengthening of the C−O bond and to a rising of the stretching force constant.[40]

Au−CO bonding in $AuCO^+$ is thought to involve some degree of $Au^+ \rightarrow$ CO π-back-donation, despite the high value of ν(CO) (ranging from 2237 cm^{-1} in a neon matrix to ~2000 cm^{-1} in $AuCO^+$ salts) that classifies the bonding as "nonclassical" under the criterion that ν(CO) is greater than its value in free CO.[41] It is recognized that, while π-back-donation weakens the CO bond and usually reduces ν(CO) to below that of free CO, its effect can be offset by the electrostatic effect of the charge on the metal interacting with the CO dipole. We attribute the decrease in ν(CO) with cluster size to charge dilution. Spreading the charge over the cluster results in a decrease in the electric field experienced by the CO and at the same time provides more electron density for back-donation. Charge dilution can also be expected to reduce the contribution of σ* donation to the Au−CO bond as the cluster becomes less electronegative; however, it has recently been shown that ν(CO) is relatively insensitive to this effect.[40] An estimate of the electrostatic contribution can be made by calculating the electric field at the CO and using comparison with the model calculations of Goldman and Krough-Jespersen[40] to predict the frequency shift relative to free CO. Assuming charge is shared among the cluster metal atoms, this model predicts that ν(CO) should drop by ~15 cm^{-1} in going from $n = 3$ to $n = 10$. The measured drop is ~40 cm^{-1}, to just below ν(CO) for free CO (Figure 6), indicating that increased π-back-bonding may also play a role in lowering ν(CO). This could especially be the case for the site responsible for the absorption at 2120 cm^{-1} in $Au_6(CO)_6^+$.

With growing cluster size one would expect ν(CO) to approach the value observed on gold surfaces. CO binds weakly to gold surfaces but can be observed in infrared reflectance measurements at low temperature and/or high CO pressure. On Au surfaces at low coverage, ν(CO) is reported in the range from 2106 to 2125 cm^{-1} for a variety of surfaces including gold films,[42] Au(110)-(1 × 2),[43,44] and oxide supported gold nanoparticles.[45] In the measurements presented here on free $Au_n(CO)_m^+$, ν(CO) is already approaching these values at $n =$ 10. If the shift due to the electrostatic effect, estimated to be about ~20 cm^{-1} is taken into account, it implies that CO binds very similarly toward bulk surfaces at low coverage and Au_n clusters with *n* as low as 10. This is consistent with earlier findings that, at low surface coverage, the preferentially occupied sites involve gold atoms with low coordination because they provide stronger CO binding.

Compilations for ν(CO) values for systems containing oxide supported gold nanoparticles have been recently given by several authors; e.g. see ref 45 and ref 46. Usually one assigns a ν(CO) absorption at 2114−2123 cm^{-1} to atop bound CO on metallic, noncharged, nanometer-sized particles. A shift toward the bulk value of 2108 cm^{-1} corresponds to formation of larger gold aggregates. Slight red shifts might be indicative of adsorption on perimeter sites of the Au particles (2090−2110 cm^{-1}).[47] Stronger red shifts are assigned to CO on small clusters perturbed by a negative charge (1950−2050 cm^{-1})[48] or attributed to bridged-bound CO (2064 cm^{-1}).[49] Strongly blue-shifted ν(CO) values are usually attributed to CO adsorbed on cationic (non-Au) sites of the support, e.g., ~2170 cm^{-1} for Fe^{3+} and ~2188 cm^{-1} for Ti^{4+}. For the intermediate range between 2120 and 2170 cm^{-1} several possible adsorption sites are under discussion, and there is some agreement that they might be due to atomic or small cluster species that are partially positively charged due to interaction with the substrate. Here, if the size of the gold species can be identified, a comparison to the ν(CO) values of the gas-phase cationic species can give an estimate of the amount of charging and thereby may provide information on the underlying substrate sites.

CO on size selectively deposited Au_8 on MgO(100) films is found to give $\nu(^{13}CO) = 2055$ cm^{-1}, implying $\nu(^{12}CO) = 2102$ cm^{-1}.[6] This is 35 cm^{-1} lower than we observe for free $Au_8(CO)_7^+$. In the Au_8/MgO system, the cluster is assumed to interact with an F-center that leads to a partially negatively charged cluster. On the basis of DFT calculations, a charging of about 0.5 e is assumed.[5] The observation of a red-shifted value for ν(CO) in comparison to the neutral, but larger, nanoparticles would be in agreement with an increased electron density at the metal. It is by no means clear that the structure of the deposited cluster matches that of the planar free cluster cation, but the inference is that the supported Au_8 cluster can provide for stronger π-back-donation than the cation.

Comparison with the Anion Complexes, $Au_n(CO)_m^-$. Our results indicate strongly that CO uptake by gold cluster cations is governed by geometric considerations based on binding site availability. Similar uptake measurements on gold anion clusters

(40) Goldman, A. S.; Krough-Jespersen, K. *J. Am. Chem. Soc.* **1996**, *118*, 12159.
(41) Lupinetti, A. J.; Fau, S.; Frenking, G.; Strauss, S. H. *J. Phys. Chem. A* **1997**, *101*, 9551.
(42) Kottke, M. L.; Greenler, R. G.; Tompkins, H. G. *Surf. Sci.* **1972**, *32*, 231.
(43) Jugnet, Y.; Cadete Santos Aires, F. J.; Deranlot, C.; Piccolo, L.; Bertolini, J. C. *Surf. Sci.* **2002**, *521*, L639.
(44) Meier, D. C.; Bukhtiyarov, V.; Goodman, D. W. *J. Phys. Chem. B* **2003**, *107*, 12668.
(45) Grunwaldt, J.-D.; Maciejewski, M.; Becker, O. S.; Fabrizioli, P.; Baiker, A. *J. Catal.* **1999**, *186*, 458.
(46) Liu, H.; Kozlov, A. I.; Kozlova, A. P.; Shido, T.; Asakura, K.; Iwasawa, Y. *J. Catal.* **1999**, *185*, 252.
(47) Boccuzzi, F.; Chiorino, A.; Tsubota, S.; Haruta, M. *J. Phys. Chem.* **1996**, *100*, 3625.
(48) Boccuzzi, F.; Chiorino, A.; Manzoli, M. *Surf. Sci.* **2000**, *454−456*, 942.
(49) Bollinger, M. A.; Vannice, M. A. *Appl. Catal. B* **1996**, *8*, 417.

note initial uptake that appears to be related to electronic shell closing in that $Au_n(CO)_m^-$ with $(n, m) = (5, 1)$, (11, 1), (15, 1), and (15, 2), corresponding to electron shell fillings at 8, 14, 18, and 20 electrons, which are preferentially formed at low CO pressures. At high CO pressure, certain $Au_n(CO)_m^-$ complexes, namely, those with $(n, m) = (7, 4)$, (9, 6), (11, 6), and (13, 6), show saturation behavior. These stoichiometries do not correspond with any obvious electronic shell closing and, unlike the cations, cannot be explained by geometric considerations based on the Au_n^- structures suggested by ion mobility measurements. There, Au_7^-, Au_9^-, and Au_{11}^- are found to have planar structures and there is no obvious geometric reason for accommodating four, six, and six CO molecules, respectively, either on these ground-state structures or on any of the reported higher lying isomers.[16]

The cations and anions do have in common the fact that the saturation CO uptake is well below that exhibited by open d-shell transition metal cluster such as Ni where CO uptake approaches the coverage predicted by electron counting rules and is limited by steric CO packing considerations.[35,36] The low CO saturation coverage of Au clusters, and how it might relate to the inactivity of bulk gold surfaces, has already been remarked on for the anions.[9] Our conclusion, based on the structures of the cationic clusters and the saturation stoichiometries, is that CO will only bind to Au atoms at room temperature if they are coordinated to less than five other Au atoms.

We are currently investigating the anion $Au_n(CO)_m^-$ complexes. These experiments should test the proposal that the favored complex stoichimetries with $(n, m) = (7, 4)$, (9, 6), (11, 6), and (13, 6) might be due to glyoxylate formation, i.e., implying C−C coupling.[9]

Conclusions

Coupled with the CO uptake measurements, the vibrational spectra of $Au_n(CO)_m^+$ complexes reveal much about the structure of both the bare clusters and the cluster complexes. Our results indicate that Au_n^+ cluster cations with $n \leq 7$ may have the planar structures suggested by ion mobility experiments. By inference we also get information on the structure of the saturated $Au_n(CO)_m^+$ complexes. In certain cases we find evidence suggesting that successive adsorption of CO can distort the metal cluster framework to accommodate additional CO ligands. The suggested structural models indicate that the CO molecules bind preferentially to gold atoms in low coordination whereas 5- and 6-fold coordinated gold atoms are not reactive toward CO. More detailed information on the structures can be expected if the infrared spectra can be simulated by DFT theory. In this regard we consider our ability to obtain spectra in the M−C stretching and M−C−O bending region especially important because of the richer structure exhibited there. We hope that this work will stimulate such studies.

Acknowledgment. We gratefully acknowledge the support of the Stichting voor Fundamenteel Onderzoek der Materie (FOM) in providing beam time on FELIX and the skill of the FELIX staff, in particular Dr. A. F. G. van der Meer and Dr. B. Redlich.

JA0509230